GEOPHYSICAL INVERSION OF HYPERSPECTRAL DATA FOR GEOLOGIC MAPPING

[*,**]**Freek van der Meer**
[*]ITC - International Institute for Aerospace Survey and Earth Sciences
Geological survey division.

[**]Delft University of Technology
Faculty of Civil Engineering and Geosciences
vdmeer@itc.nl

Key Words: Geology, mineral mapping, geophysical inversion, AVIRIS.

Abstract

Imaging spectrometer data converted to reflectance have been used successfully for mineral exploration in hydrothermal alteration systems. The common approach involves the comparison by spectral matching of known spectral signatures from spectral libraries and unknown response from a pixel. Commonly used approaches include the spectral angle mapper and spectral unmixing. These approaches have in common that mineral maps or mineral abundance maps are produced that in the end are used to derive a geologic model. In this paper we present an approach which introduces geology at the start of the processing chain. The geology is inverted to the hyperspectral data cube in an iterative manor. The sensor noise and mismatch model drives these iterations through a neural network approach. The results are interesting but not yet good; clearly more input to the models is needed.

1 Introduction

Imaging spectrometers acquire imagery in many, narrow and contiguous spectral bands with the aim of collecting "image radiance or reflectance spectra" that can be compared with field or laboratory spectra of known materials. Methods in use for the analysis of this data have in common that they quantitatively test (on a pixel by pixel basis) the similarity of unknown imaged spectra with known spectra measured in the field or laboratory or extracted from the image data at locations of known ground truth. For geological applications, this results in "mineral maps" which portray the likeness that a pixel is composed of a certain mineral. From these mineral maps, the geologist can build up a geologic model of the imaged area; thus geological knowledge is introduced at the end of the processing chain. Typical examples of such analytical approaches include the spectral angle mapper (Kruse et al., 1993) and spectral unmixing (Settle & Drake, 1993; Ichoku & Karnieli, 1996)Here an alternative approach based on geophysical inversion is presented allowing the introduction of the geologic model at the start of the processing chain. Furthermore, local knowledge is used because the inversion does not only "look" at the individual pixels but also at their surroundings or neighboring pixels. Inverse theory as commonly applied in geophysics is used, for example in the inversion of seismic waveforms, in tomography and in microwave remote sensing data.

2 Theoretical framework

In remote sensing a set of physical measurements $\{\mathbf{m}\}$ can be inverted to their resulting variables $\{\mathbf{x}\}$ if the underlying physical process is known and the following relationship is assumed

$$\mathbf{m} = \Phi(\mathbf{x}) + \mathbf{n}$$

where $\mathbf{n}$ is the sensor noise. The direct inversion in the presence of (random) noise results in

$$\mathbf{x} = \Phi(\mathbf{m})^{-1} + \mathbf{n}$$

A more flexible iterative geophysical inversion can be found with the help of a neural network based on a Bayesian approach. This neural network allows incorporating ground truth information and neighborhood information. Translating Bayes's basic theorem to our specific case we can state that in case of an all-inclusive number of independent events $\mathbf{x}_i$ that are conditionally related to the measurement $\mathbf{m}$, the probability that $\mathbf{m}$ will occur is simply

$$f(\mathbf{m}) = \sum_{i=1}^{n} f(\mathbf{m}|\mathbf{x}_i) f(\mathbf{x}_i)$$

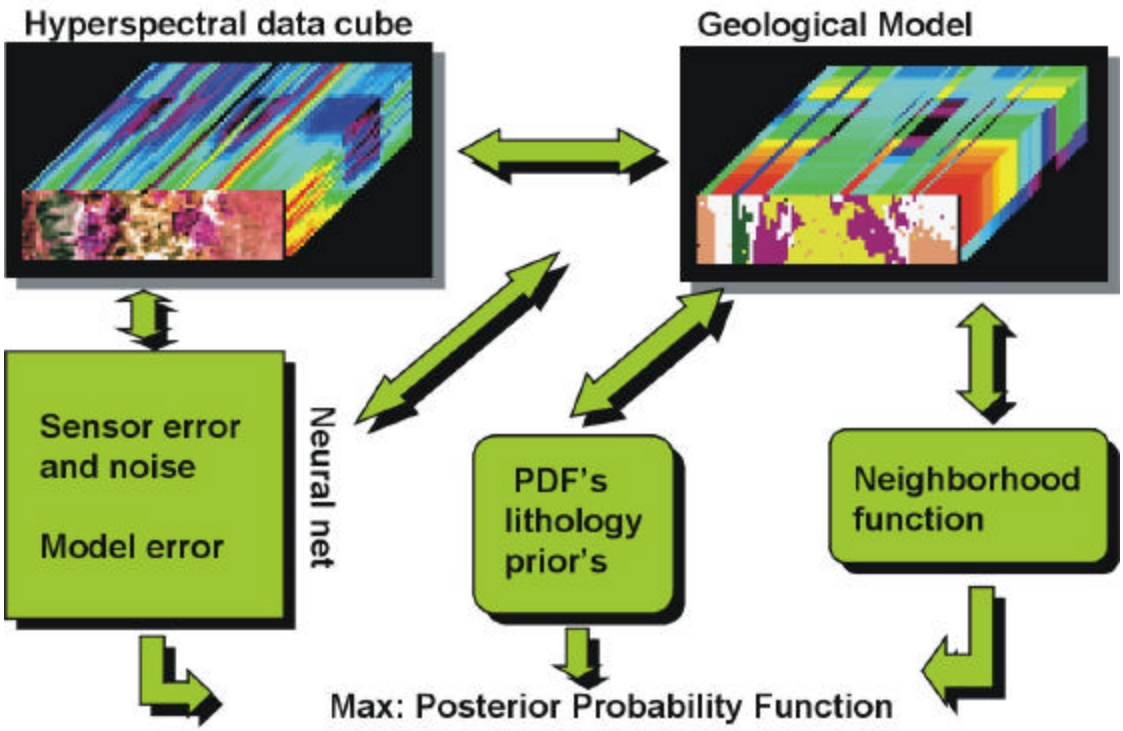

Figure 1. Schematic outline of the geophysical inversion approach.

Finding a set of parameters that maximize the observations or measurements now yield maximization of

$$\max_{\forall \mathbf{x}_i} . f(\mathbf{x}_i|\mathbf{m}) = \frac{f(\mathbf{m}|\mathbf{x}_i) f(\mathbf{x}_i)}{\sum_{i=1}^{n} f(\mathbf{m}|\mathbf{x}_i) f(\mathbf{x}_i)}$$

Note that we for the time being assume one physical measurement by the sensor (e.g., radiance or reflectance). Now let us introduce $\{\mathbf{y}\}$ as the set of parameter vectors associated with neighboring pixels. This yields the following joint probability to be maximized

$$\max_{\forall \mathbf{x}_i} . f(\mathbf{x}_i | \mathbf{m}, \mathbf{y}) = \frac{f(\mathbf{m}|\mathbf{x}_i) f(\mathbf{x}_i) f(\mathbf{y}|(\mathbf{x}_i|\mathbf{m}))}{\sum_{i=1}^{n} f(\mathbf{m}|\mathbf{x}_i) f(\mathbf{x}_i)}$$

It can be shown that this is proportional to

$$\max_{\forall \mathbf{x}_i} . f(\mathbf{x}_i | \mathbf{m}, \mathbf{y}) = f(\mathbf{m}|\mathbf{x}_i) f(\mathbf{y}|\mathbf{x}_i) f(\mathbf{x}_i)$$

Thus maximization of the conditional probability of the set of variables $\{\mathbf{x}_i\}$ given the set of measurements $\{\mathbf{m}\}$ within a neighborhood $\mathbf{y}$ is equivalent to minimizing the mismatch between (geologic-physical) model and observation (allowing some mismatch due to sensor noise), $f(\mathbf{m}|\mathbf{x}_i)$, given a prior probability, $f(\mathbf{x}_i)$, for the variables, $\mathbf{x}_i$, and a neighborhood distribution, $f(\mathbf{y}|\mathbf{x}_i)$, which is arbitrarily inferred from a kernel of 8 surrounding pixels. Figure 1 illustrates the method.

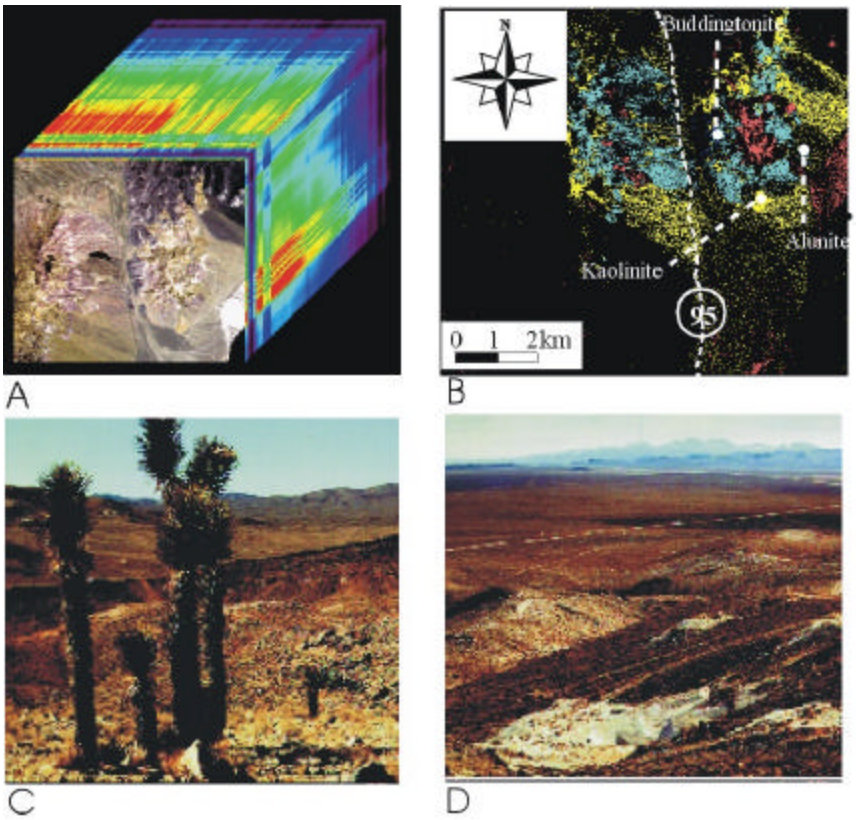

Figure 2. Images from the Cuprite mining area: (A) the AVIRIS data cube, (B) standard surface mineralogical map products, (C) view to the east, and (D) view to the north.

3 Implementation

We use 1995 AVIRIS data (Figure 2) corrected to reflectance from the Cuprite mining area situated some 30km. south of the town of Goldfield in western Nevada. The Cuprite mining site is a known area of hydrothermal alteration where in a series of rhyolitic basalt an association of the following mineral paragenesis is found:

silica ⇨ alunite ⇨ kaolinite ⇨ (buddingtonite ⇨) montmorillonite.

A spectral subset consisting of 25 spectral bands covering the clay mineral absorption features situated in the 2.1 to 2.3 micrometer range known to be diagnostic for these minerals was used from which in turn a spatial subset was extracted covering an area of intense hydrothermal alteration. For the imaged subset a geologic

model was prepared on basis of known mineral occurrences which was converted into a physical model by linking the minerals with their convoluted AVIRIS spectra. Thus the geophysical measurements {**m**} are the imaged spectra and the geophysical variables {**x**} are the geologic-physical model. The prior probability is estimated per pixel and is equivalent to expectation for the different geologic classes in the model which is simply the probability derived from the number of occurrences. The neighborhood distribution introduces within a 3-by-3 pixel kernel the geologic knowledge on the expected mineral paragenesis. If a circular zonation is assumed and the central pixel of the kernel is, for example, of the class kaolinite, than the probability that the surrounding pixels are of that same class or of either buddingtonite or alunite is higher than the probabilities of belonging to the other mineral classes. The model mismatch is taken as the difference between measurements and model at the individual pixel level. A neural network is used iteratively to reduce this mismatch by fine-tuning the geologic model. The neural network is comprised of a set of simple processing units arranged in a layered structure with a weighted connection in adjacent layers. Both the noise, *n*, and the model mismatch $f(\mathbf{x}_i) - \hat{f}(\mathbf{x}_i)$, i.e. the error between the physical measurements $f(\mathbf{x}_i)$ and the estimated geologic-physical model $\hat{f}(\mathbf{x}_i)$ by the neural network, are minimized in the process of learning by the neural network. The input layer of the neural network comprises of one unit for each discriminating variable, while the one or more hidden layers each contain a user-defined number of units. The output layer contains one unit for each geologic class.

4 Results

The model inversion was run over 9 iterations (Figure 3). Through these iterations the overall error reduces from 65% to 10% in iteration 9 (the process was stopped arbitrary at this 10% threshold level). It is clear that the noise/mismatch pattern changes from one where most of the errors or spatially correlated and can be directly related to mismatches in the geology to a random pattern possibly representing the instrument/sensor noise. The geology, however, is very much disturbed through the process where particularly the class alunite disintegrates and the classes kaolinite and montmorillonite mix up. However, the silica and buddingtonite classes are seemingly very stable throughout the process.

5 Conclusions

We have presented an interesting addition to the processing of hyperspectral data. Including the geology in the processing chain is potentially useful in bridging the gab between the remote sensing geologist and the field geologist. The geophysical inversion approach presented intends to include geological knowledge at the start of the processing chain. This as opposed to currently used algorithms for mineral mapping that build mainly on spectral matching. Hence no geological knowledge and neighborhood information is used in these models. The geophysical inversion we propose is derived from seismic processing and tomography where such approaches have been common practice for the last decades. Although theoretically sound, the results are up for improvement.

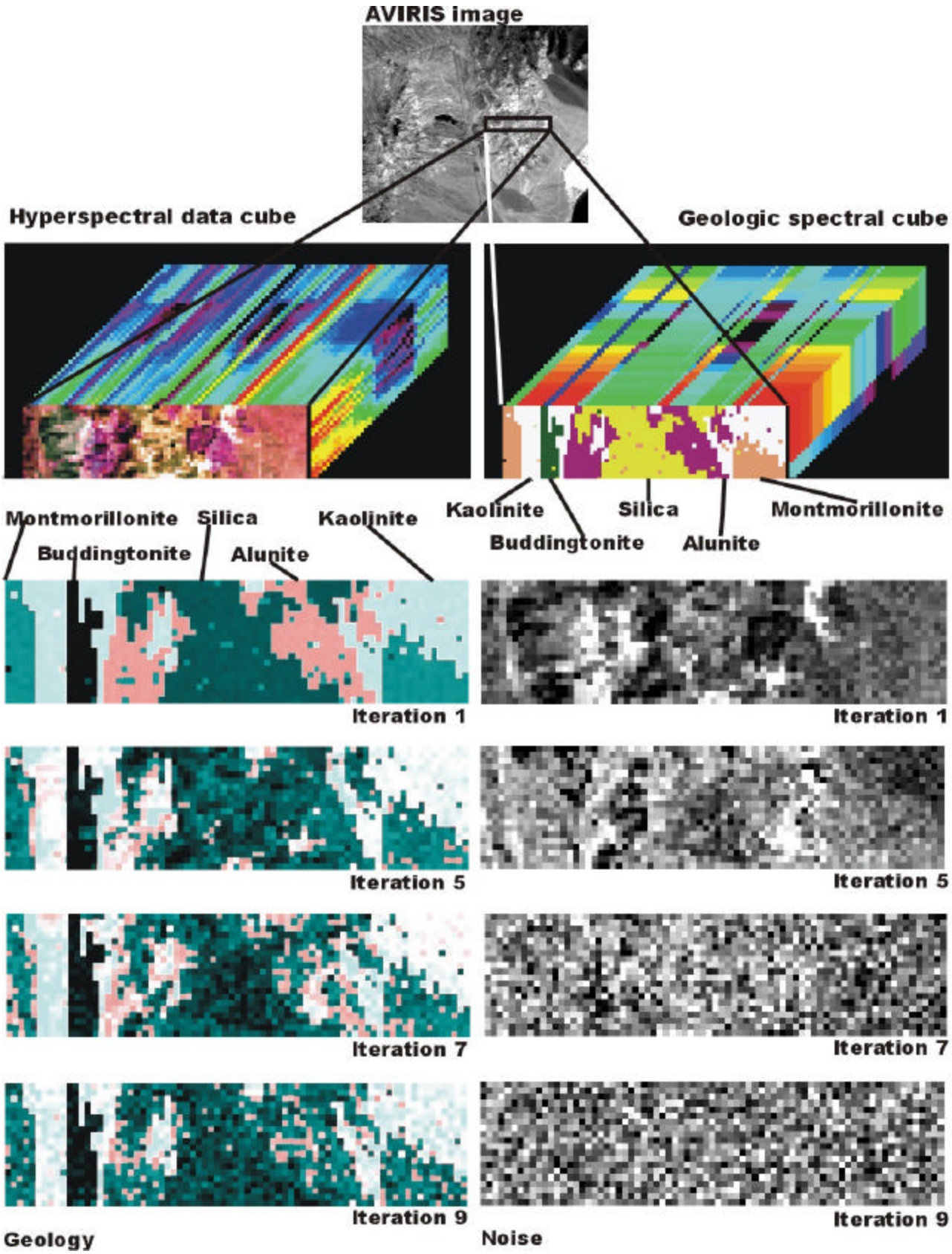

Figure 3. Results of the geophysical inversion. Left: Geology after iterations 1, 5, 7 and 9. Right: Noise model after iterations 1, 5, 7 and 9.

References

Ichoku, C. & Karnieli, A. 1996. A review of mixture modelling techniques for sub-pixel land cover estimation. Remote Sensing Reviews, 13, 161-186.

Kruse, F.A., Lefkoff, A.B., Boardman, J.W., Heidebrecht, K.B., Shapiro, A.T., Barloon, P.J. & Goetz, A.F.H. 1993. The Spectral Image Processing System (SIPS) - Interactive Visualization and Analysis of Imaging Spectrometer Data. Remote Sens. Environ., 44, 145-163.

Settle, J.J. & Drake N.A. 1993. Linear mixing and the estimation of ground cover proportions. Int. J. Rem. Sensing, 14, 1159-1177.